Emergence of metachronal waves in cilia arrays

Jens Elgeti and Gerhard Gompper[1]

Theoretical Soft Matter and Biophysics, Institute of Complex Systems and Institute for Advanced Simulation, Forschungszentrum Jülich, 52425 Jülich, Germany

Edited by T. C. Lubensky, University of Pennsylvania, Philadelphia, PA, and approved January 31, 2013 (received for review November 5, 2012)

Propulsion by cilia is a fascinating and universal mechanism in biological organisms to generate fluid motion on the cellular level. Cilia are hair-like organelles, which are found in many different tissues and many uni- and multicellular organisms. Assembled in large fields, cilia beat neither randomly nor completely synchronously—instead they display a striking self-organization in the form of metachronal waves (MCWs). It was speculated early on that hydrodynamic interactions provide the physical mechanism for the synchronization of cilia motion. Theory and simulations of physical model systems, ranging from arrays of highly simplified actuated particles to a few cilia or cilia chains, support this hypothesis. The main questions are how the individual cilia interact with the flow field generated by their neighbors and synchronize their beats for the metachronal wave to emerge and how the properties of the metachronal wave are determined by the geometrical arrangement of the cilia, like cilia spacing and beat direction. Here, we address these issues by large-scale computer simulations of a mesoscopic model of 2D cilia arrays in a 3D fluid medium. We show that hydrodynamic interactions are indeed sufficient to explain the self-organization of MCWs and study beat patterns, stability, energy expenditure, and transport properties. We find that the MCW can increase propulsion velocity more than 3-fold and efficiency almost 10-fold—compared with cilia all beating in phase. This can be a vital advantage for ciliated organisms and may be interesting to guide biological experiments as well as the design of efficient microfluidic devices and artificial microswimmers.

active matter | mesoscale hydrodynamics | dynamical self-organization

Fluid transport and locomotion due to motile cilia are ubiquitous phenomena in biological organisms on the cellular level (1, 2). Motile cilia are found in many different tissues—from the brain (3) to the lung and the oviduct—and in many uni- and multicellular organisms—from *Clamydomonas* (4) and *Volvox* (5, 6) algae to *Paramecium*. Motile cilia on the surface of a cell perform an active whip-like motion, which propels the fluid along the surface of cells and tissues. In motile cilia, the beat consists of a fast power stroke in which the cilium has an elongated shape and a slower recovery stroke in which the cilium is curved and closer to the cell surface (Fig. 1*A*). Due to their typical size in the range of 5–20 μm length and 0.25–1.0 μm thickness, the dynamics of cilia in a fluid are dominated by the balance of force generated by motor proteins (7, 8) and fluid viscosity and are thus characterized by small-Reynolds-number hydrodynamics (9). Cilia sometimes act together in pairs, such as in the breast-stroke–like motion of *Clamydomonas* (4), but much more often in large arrays, such as on the surface of *Paramecium* and *Opalina* or the tissue lining the airways of the lung. In all these cases, the beat of different cilia is not random, but strongly synchronized. For many cilia arrays, a wave-like pattern has been found and described, which is called a metachronal wave (MCW) (10). Biomimetic systems of externally actuated semiflexible strings, like chains of magnetic beads, have been proposed to use the cilia propulsion mechanism in artificial nanomachines and microfluidic devices (11–17).

Theoretical approaches to investigate hydrodynamic interactions between cilia and the formation of metachronal waves fall into three categories: (*i*) highly simplified model systems, designed to elucidate the mechanism of hydrodynamic synchronization of many active agents (18–23); (*ii*) models of an actively driven semiflexible filament, which mimic the beat of a real cilium (24–27); and (*iii*) models of a filament, with a beat shape obtained from maximizing the pumping efficiency (28, 29).

The first class of models consists either of rotors—spheres orbiting on quasi-elliptical trajectories near a wall (19–22)—or rowers—spheres that oscillate on a line with different hydrodynamic radii in the two directions of motion (18, 23)—in both cases under a constant driving force. Two rotors have been found to show asynchronous dynamics—taken as an indication for metachronal coordination—if their distance is close enough or their relative orientation is perpendicular to the beat direction (19). One-dimensional chains of such rotors (with their rotation planes parallel to the surfaces) show metachronal waves, when each rotor is given some flexibility in its motion around the anchoring point (20). One-dimensional chains of rowers also show metachronal waves under special conditions (18, 23).

The second class of models consists of semiflexible filaments, which are deformed actively by internal forces to reproduce the power and recovery strokes of real cilia and can react to the flow field generated by their neighbors (24–27, 30). The studies of such models have been restricted so far to effectively one-dimensional chains of cilia (24–27) or to 2D arrays of a small number (5×5) of cilia (30). They provide an indication of metachronal coordination, but the systems are too small or the time evolution too short to allow any prediction of MCW properties.

The third class of models also considers cilia as filaments, which are described by a chain of beads, similar to the previous case; however, the beat shape and the metachronal coordination are now determined by optimizing the pumping efficiency (28, 29). This has been done for a single cilium (29) or an array of 12×12 cilia (28). Under this assumption of maximum efficiency, MCW properties like wave direction and efficiency gain have been predicted.

Here, we present a model of independently beating cilia, which allows us to address the following questions: What is the stability of MCWs in the presence of internal or external noise? Is the wave perfect, or are irregularities and domains abundant? What are the transport properties and the efficiency gain of self-organized MCWs? How do the MCW properties depend on power-stroke direction and cilia spacing?

Model

The goal of our study is to elucidate the formation and stability of metachronal waves in large 2D cilia arrays, in which each cilium beats autonomously and is subject to internal or external noise. Thus, three aspects of ciliary beating are of fundamental importance for the construction of our computational cilium model. First, hydrodynamic interactions between cilia are the

Author contributions: J.E. and G.G. designed research; J.E. performed research; J.E. and G.G. contributed new reagents/analytic tools; J.E. analyzed data; and J.E. and G.G. wrote the paper.

The authors declare no conflict of interest.

This article is a PNAS Direct Submission.

[1]To whom correspondence should be addressed. E-mail: g.gompper@fz-juelich.de.

This article contains supporting information online at www.pnas.org/lookup/suppl/doi:10.1073/pnas.1218869110/-/DCSupplemental.

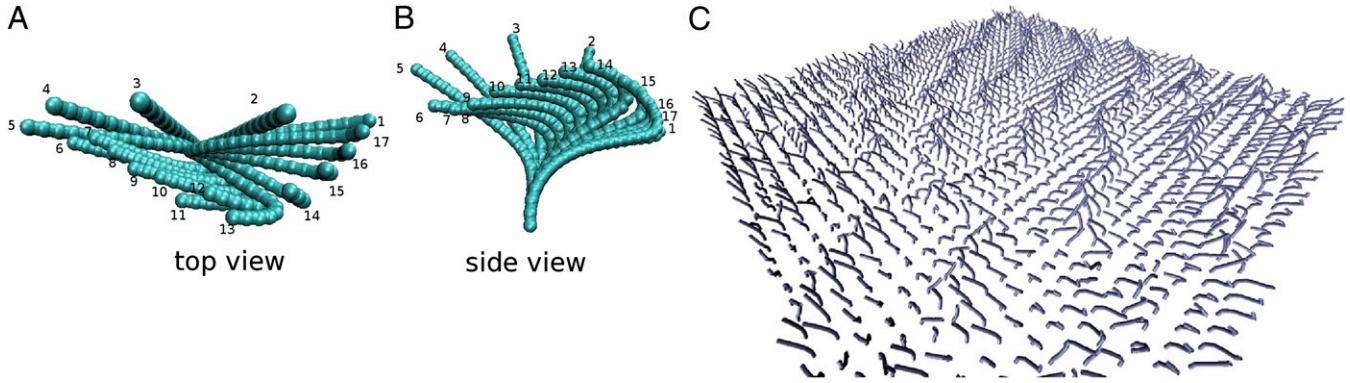

Fig. 1. (*A* and *B*) Side (*A*) and top (*B*) views of the beat pattern of the computational cilia model. Subsequent conformations are equally spaced in time. The simulated beat pattern is, for example, very similar to the beat pattern of rabbit tracheal cilia in culture medium (39). The fast, planar power stroke (frames 1–5) continues until a positive curvature threshold in the lower part of the cilium is reached. The cilium then switches to a slow, out-of-plane recovery stroke (frames 6–17), which ends when a negative curvature threshold is exceeded. See also Movie S1. A more detailed description is provided in *Materials and Methods* and in *SI Materials and Methods*. (*C*) Simulation snapshot of an array of 40 × 40 beating cilia. Cilia are placed on a square lattice, with lattice constant d_c. The metachronal wave can be easily recognized by the lines of fully extended cilia during the power stroke. See also Movie S2.

likely cause of synchronization and therefore have to be fully and consistently taken into account. Second, there are plentiful sources of noise in biological systems—ranging from thermal noise to noise in the activity of molecular motors (4, 31)—which oppose synchronization. Third, a cilium has to be able to react to the hydrodynamic forces exerted on it by its neighbors, by modifying the duration of power and recovery strokes depending on the instantaneous, local flow velocity.

We model cilia as semiflexible rods with active bending forces. For the beat pattern, we use the beat of paramecium to guide the construction of the temporal and spatial dependence of the curvature forces. The switching between power and recovery strokes and vice versa is geometry controlled, similar to the "geometric clutch hypothesis" used previously in theoretical investigations of the beat pattern of individual cilia and flagella (32). The resulting beat pattern is shown in Fig. 1 *A* and *B*.

To describe the dynamics of the surrounding fluid, we use the multiparticle collision dynamics (MPC) approach, a particle-based mesoscale hydrodynamic simulation technique that naturally includes thermal fluctuations (33, 34). We use the effective temperature inherent to our fluid-dynamics model to mimic the noise present in any biological system. In this way, we also demonstrate the robustness of our predictions to random perturbations.

Thus, in our model all cilia beat independently, with their beat reacting only to the fluid flow around them. As we impose forces, and not time-dependent cilia shapes, the beat period τ_b increases with the viscosity η. Hundreds to thousands of these model cilia are grafted on a no-slip wall, arranged in a square lattice with lattice constant d_c. The direction of the power stroke is set at an angle Θ with respect to one of the main lattice directions. A second no-slip wall closes the system two cilia lengths above. In the lateral directions we use periodic boundary conditions for the fluid motion. Alternatively, we use only a single cilium in a small box of size d_c with periodic boundary conditions to represent an infinite array of synchronously beating cilia—allowing us to identify effects of metachronal coordination. For details see *Materials and Methods* and *SI Materials and Methods*, in particular Figs. S1–S3.

Emergence of MCWs

The fundamental result of our numerical study is that all investigated cilia arrays show metachronal coordination (Fig. 1*C* and Movie S2). We initialize the system with all cilia in the same conformation. After a few beating cycles, the synchrony is quickly lost and is replaced by an essentially uncorrelated behavior. Clearly, the noise plays an important role in this quick loss of synchrony. Then metachronal coordination slowly emerges, as can be seen from the increasing size of correlated regions with time. In small arrays of 20 × 20 cilia, the correlation is in many cases so strong that the correlation length exceeds the system size. Such long-ranged correlations, despite the presence of the strong noise, demonstrate the stability of the metachronal wave. Because no other interactions (chemical or electrostatic) are present in our simulations, and neighboring cilia hardly ever come into spatial contact, hydrodynamics interaction must be the essential mechanism of synchronization.

To investigate the formation and the properties of MCWs quantitatively, we use a scalar variable to characterize the beating state of a single cilium; here, we use the projected distance of the tip from the base in the basal plane (*Materials and Methods*). Fig. 2 *A* and *B* displays snapshots of the MCW in this

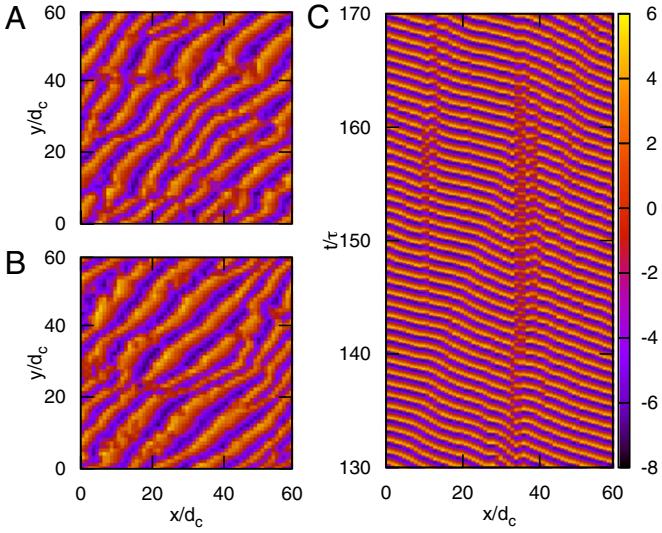

Fig. 2. (*A* and *B*) Phase-field representations of a metachronal wave, for an array of 60 × 60 cilia, at two times separated by about 40 beats. The color denotes the projected displacement of the tip of a cilium from its base in the direction of the power stroke. (*C*) Time dependence of a selected line of cilia along the *x* axis. As a function of time, defects in the metachronal wave pattern appear and disappear.

representation at fixed time and demonstrates that the wave is not perfect,but contains domains of significantly different wave lengths and propagation directions. Domains extend over several wave lengths, both parallel and perpendicular to the MCW direction. The boundary between domains shows defects similar to those of grain boundaries in imperfect crystals. Fig. 2*C* shows the temporal evolution along one spatial direction and highlights not only the persistence of domain boundaries at the same position while the MCW passes over them, but also the formation and healing of defects in the wave structure. The properties of MCWs can then be analyzed by a correlation function $G_c(\mathbf{r}, t)$ of displacement of two cilia at a relative distance $\mathbf{r}$ with time lag t. $G_c(\mathbf{r}, t)$ is found to oscillate in space and time and simultaneously to display a spatial decay (*Materials and Methods* and *SI Materials and Methods*, in particular Figs. S4–S5). In this way, many features of the metachronal wave can be extracted, such as the characteristic wave length λ, the propagation direction, the beat period τ_b, two correlation lengths ξ_1 and ξ_2, and the main correlation direction (compare Fig. 3).

For the investigation of MCW properties, we focus on the dependence on the cilia spacing d_c and the power-stroke direction (determined by the angle Θ). We find that the wave length is about two cilia lengths, $\lambda \simeq 2L_c$, depending only weakly on both d_c and Θ. This agrees well with experiments on frog esophagus (35). It is important to realize that the propagation direction of the MCW does not have to be the same as the power-stroke direction. In our cilia model, the metachronal wave propagates typically 30°–50° to the right of the power-stroke direction, nearly independent of the cilia spacing and power-stroke direction (Fig. 3). This wave direction is thus somewhere between symplectic (in the direction of the power stroke) and laeoplectic (perpendicular to the power-stroke direction) metachronism (10). An exception is the simulation with the power stroke parallel to the lattice. In this case we find antiplectic metachronism (i.e., the wave travels opposite to the power-stroke direction). We expect that the propagation direction depends significantly on the aplanarity of the beat pattern (Fig. 1*A*).

The main correlation direction is determined by the direction of slowest decay of the correlation function $G_c(\mathbf{r}, t)$. In the simulations, it is found to be roughly parallel to the power-stroke direction, see Fig. 3, in agreement with observations for frog esophagus (35). The main correlation direction depends very weakly on cilia spacing; some small systematic deviation can be seen in Fig. 3, which we attribute to interplay of the metachronal wave with the high-symmetry directions of the square lattice.

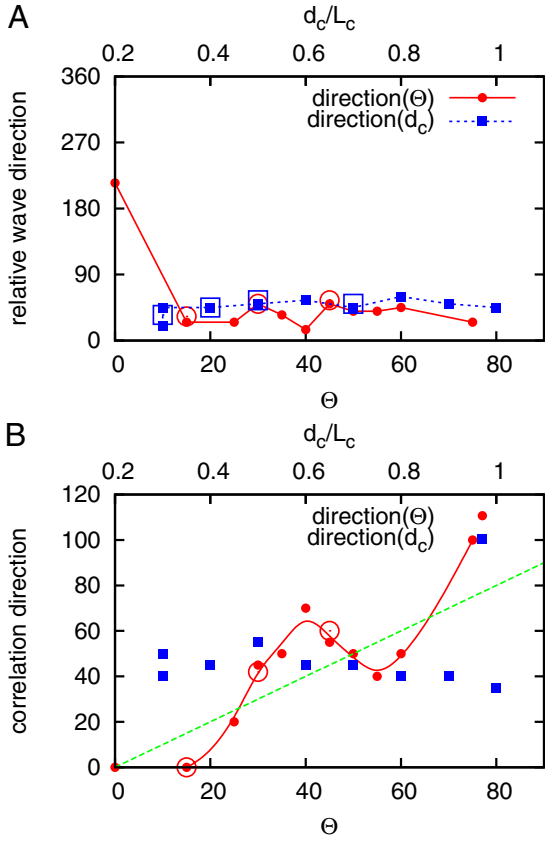

Fig. 3. (*A* and *B*) Wave direction relative to the power-stroke direction (*A*) and the main correlation direction (*B*), as a function of power-stroke direction Θ (lower axis) and cilia spacing d_c (upper axis). Large open symbols indicate larger systems of 60 × 60 cilia, and small solid symbols show smaller systems of 20 × 20 cilia. The green line indicates where the main correlation direction equals the power-stroke direction.

Transport

Transport and Beating Period. We now turn our attention to fluid transport, the main function of cilia. Because the beat period τ_b is the dominant timescale, the transport velocity can be expected to scale with the beat frequency. This has been shown experimentally for mucus-propelling cilia (36). We thus first discuss the beat period in more detail (Fig. 4*A*). The simulations show that τ_b of synchronously beating cilia decreases with decreasing cilia spacing, whereas τ_b of cilia in metachronal coordination increases. With increasing cilia distance, the difference between beat frequencies with and without metachronal coordination decreases, until τ_b is independent of metachronal coordination for large distances $d_c/L_c \gtrsim 1.0$. Furthermore, we note that the SD of the period is by far smaller for synchronously beating cilia then for cilia in metachronal coordination (Fig. 4). The physical origin of these behaviors is discussed in the *Interpretation* section.

Transport Velocity. A simple picture of an array of periodic rowers would now suggest that the transport velocity is proportional to the beat frequency and the cilia density. The observed fluid transport velocities, shown in Fig. 4*B*, come thus as a surprise, because they show a much larger velocity for MCWs compared with synchronous beating although the beat frequency in MCWs is reduced. The metachronal gain, the increase of fluid transport velocity due to metachronal coordination, would thus be even larger if the same beat frequency were maintained. The transport velocity is essentially independent of metachronal coordination for "large" cilia separations $d_c \simeq L_c$. For cilia that are packed more closely, fluid transport is faster, as expected. However, this effect is much stronger for metachronally coordinated cilia. This results in an enhancement of almost a factor of 3 in fluid velocity between metachronal and synchronous beating cilia for the smallest investigated cilia spacing of $d_c/L_c = 0.3$. The data in Fig. 4*B* for the dependence of the transport velocity v on the cilia distance d_c are well described by a power-law decay,

$$v \sim d_c^{-\alpha}. \qquad [1]$$

Fits of this dependence to the simulation data in the range $0.3 \le d_c/L_c \le 1.0$ yield $\alpha = 1.4$ for MCWs in arrays of 20 × 20 cilia and $\alpha = 0.6$ for synchronously beating cilia.

Transport Efficiency. The reduced beat frequency and increased fluid velocity imply a markedly enhanced transport efficiency of cilia with metachronal coordination. We define a dimensionless efficiency ϵ as the ratio of the cilia energy consumption P_c per

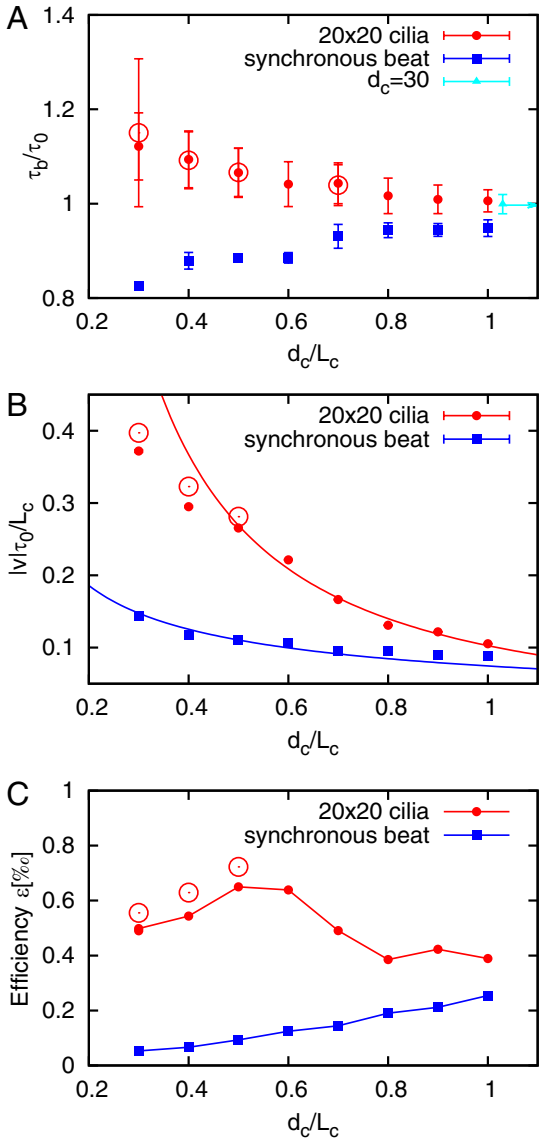

Fig. 4. (*A*) Beat period τ_b vs. cilia spacing d_c. Small red symbols indicate results for MCWs in arrays of 20 × 20 cilia and large red symbols those in arrays of 60 × 60 cilia. Blue symbols indicate results for synchronously beating cilia. The data point marked by the light blue symbol is obtained for synchronously beating cilia with $d_c = 30$. Error bars denote SD. (*B*) Average fluid velocity v as function of cilia spacing d_c for cilia in metachronal coordination (red) and corresponding synchronously beating cilia (blue). Solid lines are fits to Eq. **1** (using data for $d_c \geq 5$ with 20 × 20 cilia). (*C*) Dimensionless efficiency ϵ as a function of cilia spacing d_c, as indicated for systems of 20 × 20 cilia and synchronously beating cilia.

unit time and the power required to obtain the same average velocity with a constant driving-force density in a film of the thickness L_c as the cilia length, at a (single) no-slip wall in a semiinfinite system. This implies that

$$\epsilon = \frac{16}{3}\frac{\eta v^2 d_c^2}{L_c P_c} \qquad [2]$$

(details in *SI Materials and Methods*, in particular Fig. S6), in agreement with the functional form of the efficiency used in refs. 28 and 29. As the energy consumption per cilium per beat, ΔE, is roughly independent of cilia spacing, we obtain approximately $P_c \simeq \Delta E/\tau_b$. The efficiency as a function of cilia spacing is shown in Fig. 4*C*. Because cilia in MCWs beat slower, and propel the fluid faster, the efficiency increases up to 10-fold through metachronal coordination. The optimal efficiency is found at a cilia spacing of about $0.5L_c$ for metachronally coordinated cilia. In the limit of large d_c, the efficiency is expected to be independent of the cilia coordination.

Interpretation. Next we discuss the physical origin of the observed behavior of MCWs. The increasing transport velocity with decreasing cilia spacing can be understood from simple scaling arguments. As a strongly simplified model, we consider again Poiseuille-like flow, which is driven by a constant force density g (per unit volume) in a layer of thickness L_c near a no-slip wall. This model yields an average transport velocity $v = gL_c^2/(4\eta)$ and power consumption per unit area $P_c/d_c^2 = g^2L_c^3/(3\eta)$ (*SI Materials and Methods*). To proceed, we need to relate the cilia action to the driving force in the Poiseuille-like flow. A reasonable assumption is that each cilium generates a constant total pushing force F_c, which is homogeneously distributed over the volume $d_c^2L_c$, which implies

$$v \sim (F_c L_c/\eta) d_c^{-2}. \qquad [3]$$

Alternatively, we can assume that each cilium works at a constant total power output ϵP_c. Because $P \sim Fv$, this implies that at higher velocities, the cilia exert a lower force. For the Poiseuille-like case, this yields

$$v \sim (P_c L_c/\eta)^{1/2} d_c^{-1}. \qquad [4]$$

Because the simulation results are reasonably well described by the exponents $\alpha = 1.4$ and $\alpha = 0.6$ for systems with and without MCWs, respectively, we conclude that cilia in MCWs are more able to exert their full force on the fluid than synchronously beating cilia. The exponent $\alpha > 1$ for MCWs indicates that the cilia actually create (on average) a larger power output the closer they are packed, in contrast to synchronously beating cilia.

Why are cilia in metachronal coordination more able to exert their full force than synchronously beating cilia? Clearly this is an effect of correlations. When the distance between cilia is large, hydrodynamic interactions (HI) become unimportant, so that the beat period and transport are independent of metachronal coordination. As d_c decreases, the effect of HI on synchronously beating cilia is different from the effect on cilia in metachronal coordination. Synchronously beating cilia facilitate the beat of their neighbors through hydrodynamic interactions, because the flow field they generate points in the same direction as the beat. Although this results in faster movement—explaining the observed decrease of the beat period (Fig. 4*A*)—it also implies that only a fraction of the force can be converted into forward fluid

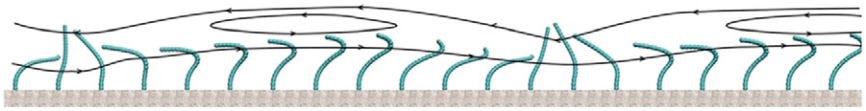

Fig. 5. Schematic view of metachronal beating to explain the origin of metachronal gain.

motion. Like a cyclist in too low gear, pedaling is fast, but inefficient. Furthermore, a large part of the fluid is just moving back and forth. This causes larger local shear rates and thus more energy dissipation.

On the other hand, a cilium in metachronal coordination feels an opposing flow of its neighbors, slowing down the beat (Fig. 5 shows a schematic view). During both power and recovery strokes, the cilia feel an opposing flow generated by the neighboring cilia. First, this implies that cilia beat slows down with decreasing d_c, consistent with the increase in beat period (Fig. 4*A*) (the increased SD of the beat period τ_b in MCWs can be traced back to the significant modification of the beat pattern of individual cilia within an MCW, whereas the beat pattern of synchronously beating cilia is stabilized by the identical beat of the neighbors). Second, working against the opposing flow of their neighbors, cilia in MCWs are able to exert a large force on the fluid, which implies a better velocity scaling; compare Eq. **3**. These arguments qualitatively explain the observed beat frequencies, fluid velocities, and transport efficiency.

Discussion

It is now interesting to compare the results of our self-organized MCW model with the results of the "optimized-efficiency" model of ref. 28. We stress that the model of ref. 28 is based on the very strong assumption that the shape and time dependence of the cilia beat are governed by the search for optimum efficiency. In contrast, our approach starts from a self-generated beat of a single cilium, which then adapts to the fluid-mediated forces by the other cilia. We address three points. First, the dependence of the average fluid velocity on the cilia spacing can be extracted from the efficiency data presented in ref. 28; here, a fit to an effective power law yields $\epsilon \sim (d_c/L_c)^{-1.25}$, which corresponds to a velocity $v \sim \sqrt{\epsilon} L_c/d_c \sim d_c^{-1.6}$ (obtained from Eq. **2** for constant P_c). Somewhat surprisingly, this is quite comparable to our velocity decay $v \sim d_c^{-1.4}$. Second, a comparison of the absolute efficiency shows that the efficiency of our model is at least an order of magnitude smaller than that of the model of ref. 28. Several factors contribute to the reduction of efficiency, such as (*i*) the internal dissipation of our cilia, (*ii*) the not efficiency-optimized beat of our cilia, in particular the larger distance of the flagellum from the wall during the recovery stroke, (*iii*) some slip of the fluid on the cilia, (*iv*) defects in the MCW (Fig. 2), and (*v*) the presence of a second wall at distance $2L_c$ (whereas a semiinfinite fluid was considered in ref. 28). However, when the efficiency gain is compared for $d_c/L_c = 1$ (the only cilia distance where this information is available in ref. 28), we find a quite similar factor of 2.0 for our model to 3.5 for the optimized-efficiency model. Third, and finally, for the case of flow direction equaling lattice direction studied in ref. 28, the MCW is predicted to be antiplectic, in agreement with our results for $\Theta = 0$. However, the data for our model presented in Fig. 3 show that $\Theta = 0$ is a rather special case, because for all other cases we find a wave that is between symplectic and laeoplectic. It is interesting to note that the results of the optimized-efficiency model for $\Theta = 0$ indicate that symplectic waves are nearly as efficient as antiplectic waves. It would be interesting to see whether symplectic waves can also be obtained in the optimized-efficiency model for flow directions differing from the main lattice direction.

Conclusions and Outlook

In summary, our results provide insight into the mechanism of cilia-driven transport. The modeling framework presented here can be extended in the future to understand other cilia-related transport phenomena and swimming of ciliated microorganisms. It can also be used to study and understand the cellular origins of cilia-dysfunction–related diseases (37). In particular, we hope that our results will stimulate biological experiments to study the dependence of MCW properties on cilia spacing. In systems of artificial cilia (11–14, 16, 17), the main obstacle so far for the self-organized formation of MCWs is the need for an internal feedback of the cilia beat on the local flow conditions. We hope that our results will contribute to the design of new autonomous cilia-like rowers, which have this important property.

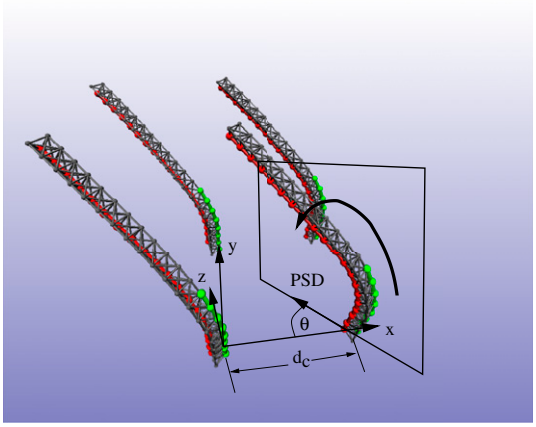

Fig. 6. Each cilium is modeled by three semiflexible filaments consisting of chains of monomers that are connected by harmonic springs of length $_b$ (nearest neighbors) and $_c$ (next-nearest neighbors) to form a crane-like structure. Bond lengths are varied to induce a preferred curvature. The bond lengths of the "red" filament are varied to create the power and recovery strokes. In addition, the preferred bond lengths of the seven bonds at the base of the "green" filament are stretched by 10% to generate aplanarity during the recovery stroke. The power-stroke direction (PSD) is rotated by an angle Θ with respect to the main lattice direction.

Materials and Methods

A detailed description of the model, methods, and results is given in *SI Materials and Methods*. A brief summary is given below.

Model. We use a mechanistic, 3D model of a cilium, which is designed to capture the active beat and the hydrodynamics of interacting cilia arrays. Each cilium is represented by a bundle of three parallel semiflexible filaments, each of which consists of a linear chain of beads and springs (Fig. 6); the filaments are interconnected by a second type of spring to keep them approximately at a fixed distance from each other (38). For activity, a dynamic spontaneous curvature is created by locally varying the lengths of springs of one of the three filaments. This mechanism is inspired by the connecting dynein motors moving along adjacent microtubules in the axoneme—including the effect of a stall force. During the power stroke, the force distribution along the cilium is adjusted such that a nearly straight, extended conformation is achieved. In the recovery stroke, the force distribution is constructed such that a strongly curved part travels from the anchoring part of the cilium to its free end. For MCWs to develop, a feedback between the hydrodynamic flow and the beat pattern is essential. Motivated by the "geometric clutch hypothesis" (32), we assume that switching between power and recovery strokes is controlled by curvature thresholds of the individual cilium; i.e., no external clock is used to determine the beat pattern. The power-stroke direction (PSD) forms an angle Θ with the main lattice direction, as illustrated in Fig. 6.

Correlation Function. To characterize MCWs, we define the phase of the beat of an individual cilium by $B = \cos(\Theta)\Delta x + \sin(\Theta)\Delta y$, where $\Delta x = x(tip) - x(base)$ and $\Delta y = y(tip) - y(base)$ are the projected displacements of the tip of the cilium from its base, and Θ is the power-stroke direction. This defines the phase field $B(r, t)$, where r is

$$G_c(r,t) = \langle \delta B(r_0,t_0)\delta B(r_0+r,t_0+t)\rangle_0 / \langle \delta B(r_0,t_0)^2\rangle, \quad [5]$$

where $\delta B(r_0, t_0) = B(r_0, t_0) - B(r_0, t_0)$, and the average is taken over all lattice positions r_0 and over a time interval of about 10 beat periods. After some initial time interval, correlations are very well described by the functional form

$$G_c(r,t) = \cos(k\cdot r - \omega t)[(1-c_1)\exp(-\sqrt{r\chi r}) + c_1]. \quad [6]$$

The fitted parameters are the wave vector k, the correlation matrix χ (where

χ is a 2×2 matrix, with the two eigenvalues $1/\xi_1^2$ and $1/\xi_2^2$), the beat frequency ω, and a long-range order parameter c_1. These quantities allow a detailed characterization of the metachronal wave. This scheme should also be well suited for the analysis of experimental data.

1. Bray D (2001) *Cell Movements: From Molecules to Motility* (Garland, New York), 2nd Ed.
2. Alberts B, et al. (2007) *Molecular Biology of the Cell* (Garland, New York), 5th Ed.
3. Sawamoto K, et al. (2006) New neurons follow the flow of cerebrospinal fluid in the adult brain. *Science* 311(5761):629–632.
4. Goldstein RE, Polin M, Tuval I (2009) Noise and synchronization in pairs of beating eukaryotic flagella. *Phys Rev Lett* 103(16):168103.
5. Short MB, et al. (2006) Flows driven by flagella of multicellular organisms enhance long-range molecular transport. *Proc Natl Acad Sci USA* 103(22):8315–8319.
6. Drescher K, Goldstein RE, Tuval I (2010) Fidelity of adaptive phototaxis. *Proc Natl Acad Sci USA* 107(25):11171–11176.
7. Brokaw CJ (1972) Computer simulation of flagellar movement. I. Demonstration of stable bend propagation and bend initiation by the sliding filament model. *Biophys J* 12(5):564–586.
8. Camalet S, Jülicher F, Prost J (1999) Self-organized beating and swimming of internally driven filaments. *Phys Rev Lett* 82:1590–1593.
9. Purcell EM (1977) Life at low reynolds-number. *Am J Phys* 45:3–11.
10. Sleigh MA (1962) *The Biology of Cilia and Flagella* (Pergamon, Oxford).
11. Dreyfus R, et al. (2005) Microscopic artificial swimmers. *Nature* 437(7060):862–865.
12. Kim YW, Netz RR (2006) Pumping fluids with periodically beating grafted elastic filaments. *Phys Rev Lett* 96(15):158101.
13. Gauger EM, Downton MT, Stark H (2009) Fluid transport at low Reynolds number with magnetically actuated artificial cilia. *Eur Phys J E Soft Matter* 28(2):231–242.
14. Branscomb J, Alexeev A (2010) Designing ciliated surfaces that regulate deposition of solid particles. *Soft Matter* 6:4066–4069.
15. Vilfan M, et al. (2010) Self-assembled artificial cilia. *Proc Natl Acad Sci USA* 107(5): 1844–1847.
16. Sanchez T, Welch D, Nicastro D, Dogic Z (2011) Cilia-like beating of active microtubule bundles. *Science* 333(6041):456–459.
17. Sareh S, Rossiter J, Conn A, Drescher K, Goldstein RE (2013) Swimming like algae: Biomimetic soft artificial cilia. *J R Soc Interface* 10(78):20120666.
18. Cosentino Lagomarsino M, Jona P, Bassetti B (2003) Metachronal waves for deterministic switching two-state oscillators with hydrodynamic interaction. *Phys Rev E Stat Nonlin Soft Matter Phys* 68(2 Pt 1):021908.
19. Vilfan A, Jülicher F (2006) Hydrodynamic flow patterns and synchronization of beating cilia. *Phys Rev Lett* 96(5):058102.
20. Niedermayer T, Eckhardt B, Lenz P (2008) Synchronization, phase locking, and metachronal wave formation in ciliary chains. *Chaos* 18(3):037128.
21. Uchida N, Golestanian R (2010) Synchronization and collective dynamics in a carpet of microfluidic rotors. *Phys Rev Lett* 104(17):178103.
22. Golestanian R, Yeomans JM, Uchida N (2011) Hydrodynamic synchronization at low reynolds number. *Soft Matter* 7:3074–3082.
23. Wollin C, Stark H (2011) Metachronal waves in a chain of rowers with hydrodynamic interactions. *Eur Phys J E Soft Matter* 34(4):1–10.
24. Gueron S, Levit-Gurevich K, Liron N, Blum JJ (1997) Cilia internal mechanism and metachronal coordination as the result of hydrodynamical coupling. *Proc Natl Acad Sci USA* 94(12):6001–6006.
25. Gueron S, Levit-Gurevich K (1999) Energetic considerations of ciliary beating and the advantage of metachronal coordination. *Proc Natl Acad Sci USA* 96(22):12240–12245.
26. Guirao B, Joanny JF (2007) Spontaneous creation of macroscopic flow and metachronal waves in an array of cilia. *Biophys J* 92(6):1900–1917.
27. Yang X, Dillon RH, Fauci LJ (2008) An integrative computational model of multiciliary beating. *Bull Math Biol* 70(4):1192–1215.
28. Osterman N, Vilfan A (2011) Finding the ciliary beating pattern with optimal efficiency. *Proc Natl Acad Sci USA* 108(38):15727–15732.
29. Eloy C, Lauga E (2012) Kinematics of the most efficient cilium. *Phys Rev Lett* 109(3): 038101.
30. Gueron S, Levit-Gurevich K (2001) A three-dimensional model for ciliary motion based on the internal 9+2 structure. *Proc Biol Sci* 268(1467):599–607.
31. Drescher K, Dunkel J, Cisneros LH, Ganguly S, Goldstein RE (2011) Fluid dynamics and noise in bacterial cell-cell and cell-surface scattering. *Proc Natl Acad Sci USA* 108(27):10940–10945.
32. Lindemann CB (2004) Testing the geometric clutch hypothesis. *Biol Cell* 96(9):681–690.
33. Kapral R (2008) Multiparticle collision dynamics: Simulation of complex systems on mesoscales. *Adv Chem Phys* 140:89–146.
34. Gompper G, Ihle T, Kroll DM, Winkler RG (2009) Multi-particle collision dynamics – a particle-based mesoscale simulation approach to the hydrodynamics of complex fluids. *Adv Polym Sci* 221(1):1–87.
35. Gheber L, Priel Z (1994) Metachronal activity of cultured mucociliary epithelium under normal and stimulated conditions. *Cell Motil Cytoskeleton* 28(4):333–345.
36. Braiman A, Priel Z (2008) Efficient mucociliary transport relies on efficient regulation of ciliary beating. *Respir Physiol Neurobiol* 163(1–3):202–207.
37. Fliegauf M, Benzing T, Omran H (2007) When cilia go bad: Cilia defects and ciliopathies. *Nat Rev Mol Cell Biol* 8(11):880–893.
38. Elgeti J, Kaupp UB, Gompper G (2010) Hydrodynamics of sperm cells near surfaces. *Biophys J* 99(4):1018–1026.
39. Sanderson MJ, Sleigh MA (1981) Ciliary activity of cultured rabbit tracheal epithelium: Beat pattern and metachrony. *J Cell Sci* 47:331–347.